Polymer Chemistry

Accepted Manuscript

ROYAL SOCIETY OF CHEMISTRY

www.rsc.org/polymers

Cite this: DOI: 10.1039/c0xx00000x

www.rsc.org/xxxxxx

Communication

One-Pot Synthesis of Indolizine Functionalized Nanohyperbranched Polyesters with Different Nano Morphologies and their Fluorescent Response to Anthracene

Xiaoxia Wang[1], Fanyang Zeng[1], Can Jin[2], Yuliang Jiang[1], Qiaorong Han[1*], Bingxiang Wang[1]* and Zhenye Ma[1]*

Received (in XXX, XXX) Xth XXXXXXXXX 20XX, Accepted Xth XXXXXXXXX 20XX

DOI: 10.1039/b000000x

The structurally controllable hyperbranched HBPE-CIDAs (HBPE modified with CIDA units) were synthesized by modifying periphery of the second generation hyperbranched polyester (HBPE) with 1-cyanoindolizine-3-carboxylic acid (CIDA) groups *via* a one-pot synthesis. The structures and self-assembly behaviors of HBPE-CIDAs were established by combined studies of FFT-IR, NMR, TEM, SEM, AFM and XRD. Furthermore, host-guest recognition of HBPE-CIDAs were investigated by fluorescent studies. The results indicated that the HBPE-CIDA$_4$ nanospindles have weaker response to various metal ions while better selectivity to anthracene through π-π stacking interactions than the HBPE-CIDA$_1$ nanospheres.

During the past decades, hyperbranched polymers (HBPs) have attracted extensive interest due to their unique chemical and physical properties.[1-13] As one class of architectural macromolecules, HBPs could be readily synthesized in a one-pot procedure in contrast to regular dendrimers, as a result, their nature of the backbone, the chain-end functional groups, degree of branching, chain length between branching points, and the molecular weight distribution could be modified easily for specific purpose. Moreover, the self-assembly of hyperbranched copolymers in the form of fibers,[14-16] nanotubes,[17, 18] zigzags,[19-21] rod,[22, 23] helices[24, 25] and necklace[26] indicate that the architecture and composition of the copolymers play extremely critical roles in determining micellar morphology, since they affect the conformational packing geometry of micellar structures. In order to further understand the structure-property correlation and explore novel self-assembled structures, much efforts has been made to develop the hyperbranched polymers with novel chemical structure and topological architecture. Nevertheless, to date, assemblies of hyperbranched polymers, which could be engineered to obtain supramolecular assemblies with combined or enhanced properties, remain challenging and have only been addressed by a few studies.[27-31] Therefore, hyperbranched polymer self-assembly has been an area of intense research, not only out of academic interest but also for their potential applications.

A variety of molecular designs have been proposed recently for the fabrication of nanostructured hyperbranched polyesters (HBPE, one imports family of HBPs) leading to multifunctional macromolecule materials.[32-38] For example, Zhu and Zhou reported the multifunctional hyperbranched polyester-based nanoparticles and nanocomposites with properties ranging from biomedical fields, nanotechnology and fluorescence functional materials.[39, 40] Our group developed the hyperbranched polyester nanorods with pyrrolo[2,1-a]isoquinoline end-groups.[23] However, to the best of our knowledge, there have not yet been any study on the formation of organized spindle-like nano morphology and nanospheres in one-pot procedure from hyperbranched molecules composed of irregular, random branched fragments with the degree of branching well below that observed for the dendrimer architecture,[41-43] most likely because generally hyperbranched molecules are not expected to form regular one dimensional supramolecular nanospindle structures owning to their high polydispersities, irregular architectures, and poorly defined shapes. Most of the reported hyperbranched polymers with different nano morphologies were all formed by changing the tested conditions with the same sample,[3, 4, 44-48] while two samples with different nano morphologies synthesized by a one-pot procedure has not been explored.

Most recently, our group demonstrated two interesting 1-cyanopyrrolo[2,1-a]isoquinoline 3-carboxylic acid (CICA) modified HBPE with the same backbone while different grafting rates (2 and 6, respectively), so-called HBPE-CICAs, showed similar rod-like nano morphologies.[23] We assumed that the highly conjugated structure of the peripheral groups resulting in strong π-π stacking with HBPE backbone might, at least partially, contribute to their similar rigid nano morphologies. To develop diverse nano morphologies and considering that indolizine derivatives exhibit a wide array of biological activities[49] and the high fluorescence quantum yield,[50] herein we designed and synthesized a novel class of hyperbranched aromatic-aliphatic co-polyester HBPE-CIDAs with the 1-cyanoindolizine-3-carboxylic acid (CIDA, one benzene ring less than previous CICA) as their peripheral groups.

As expected, we obtained two products with different grafting rates *via* one-pot synthesis method, which exhibited spherical and spindle-like nano morphologies, respectively. In addition, we

investigated the host-guest recognition properties with fluorescence study of these functionalized HBPE-CIDA nanoparticles in presence of various metal cations and some of fused ring compounds in solution.

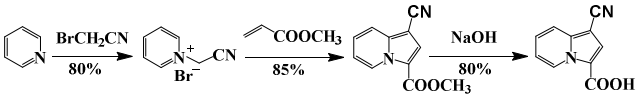

Scheme 1 Synthetic route of CIDA

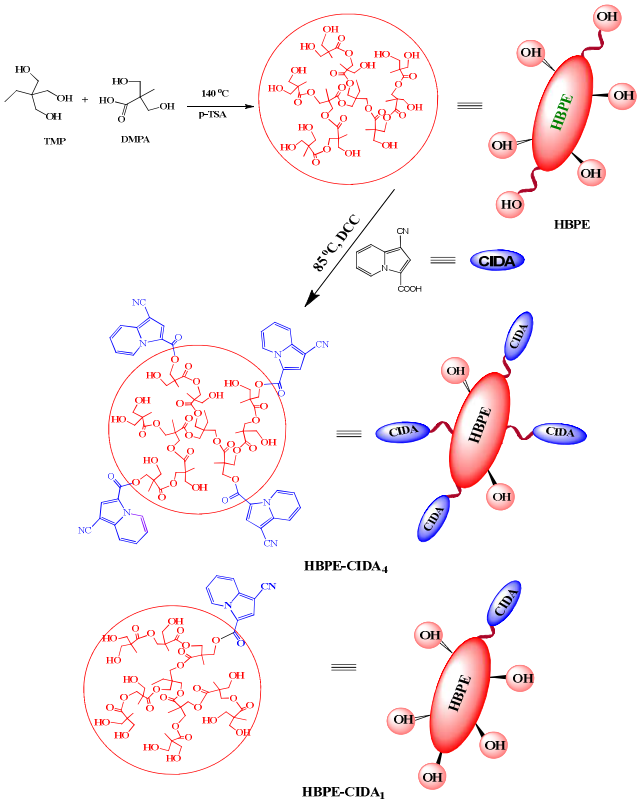

Scheme 2 Synthetic routes of HBPE, HBPE-CIDA$_1$ and HBPE-CIDA$_4$ (in order to simplify the cartoon pictures, half of the periphery –OH groups of HBPE were omitted).

1-cyanoindolizine-3-carboxylic acid (CIDA) was synthesized by a three-step procedure (Scheme 1) and its structure was confirmed by combination of IR (Fig. 1), ^{1}H NMR (Fig. 2) and ESI-MS spectra (Fig. S1 in Supporting Information). The synthetic route of HBPE was described as Scheme 2 and the synthesis method was described in the Supporting Information.

The HBPE-CIDAs were synthesized as shown in Scheme 2. Accordingly, to a solution of HBPE (0.12 g, 0.10 mmol) and CIDA (0.24 g, 1.3 mmol) in DMSO (60 mL), *N, N'*-dicyclohexyl carbodimide (DCC, 0.29 g, 1.39 mmol) was added. The mixture was heated at 85 °C under nitrogen for 20 hours. The resulting solution was evaporated, and the residue was poured into ethyl acetate (60 mL), then filtered. The filtrate was concentrated and subjected to column chromatography (silica gel, eluent: ethyl acetate/petroleum ether = 1/2). Two yellow bands were collected and evaporated, which were identified later as HBPE-CIDA$_1$ and HBPE-CIDA$_4$ in yields of 50% and 30%, respectively.

The structures of modified hyperbranched polyester HBPE-CIDA$_1$ and HBPE-CIDA$_4$ were initially established by FT-IR as shown in Fig. 1. The FT-IR spectra of HBPE-CIDA$_1$ and HBPE-CIDA$_4$ were found to be quite similar to those of CIDA and HBPE. All of them showed similar characteristic peaks of indolizine ring at 1572, 1533 and 1445 cm^{-1}; signals of C=O at 1670 cm^{-1} and 1631 cm^{-1}; signals of -C-O-C- at 1240 cm^{-1}. The characteristic peaks of -CN at 2354 cm^{-1} were obviously observed only for CIDA, HBPE-CIDA$_1$ and HBPE-CIDA$_4$ (black, red and blue curves, respectively), while not for unmodified HBPE (green curve).

^{1}H NMR (Fig. 2) spectra further confirmed the chemical composition of the modified compound HBPE-CIDA$_1$ and HBPE-CIDA$_4$. Signals at 6.97–9.63 ppm were attributed to the modified end-groups (CIDA). Protons of $R_3CCOOCH_2$ and $ArCOOCH_2$ could be observed at 4.14 and 4.26 ppm, respectively, while those of methyl groups appeared at 0.83–1.63 ppm. Moreover, the CIDA grafting of HBPE-CIDA$_4$ and HBPE-CIDA$_1$ could be calculated by integration ratio of the aromatic protons (**b**) and alphatic protons (**a**) (CH_3- of the CH_3CH_2-groups) with the formula ($S_b/(20S_a)$) were about 30.5% and 8.5%, respectively, which indicated that four peripheral CIDA groups were grafted to the former product while only one CIDA to the later. Therefore we named these two products as HBPE-CIDA$_4$ and HBPE-CIDA$_1$.

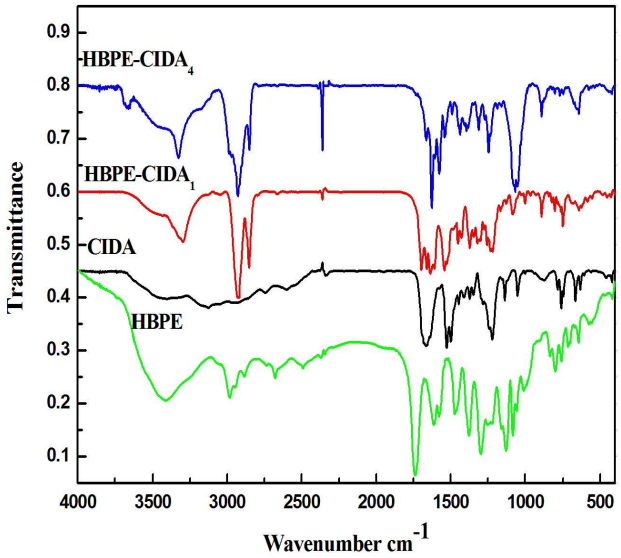

Fig. 1 FT-IR spectra of CIDA (blue line), HBPE (green line), HBPE-CIDA$_1$ (black line) and HBPE-CIDA$_4$ (red line)

In addition, the MALDI-MS (m/z) of HBPE-CIDA$_1$ (1347.3, Fig. S5 in Supporting Information) and HBPE-CIDA$_4$ (1852.3, Fig. S6) were consistent with those calculated values (1347.7 and 1851.7, respectively). The ^{13}C NMR spectra of HBPE-CIDA$_1$ and HBPE-CIDA$_4$ were illustrated in Fig. S4.

Transmission electron microscope (TEM) experiments were performed to estimate the sizes and morphologies of HBPE-CIDA$_1$ and HBPE-CIDA$_4$. As shown in Fig. 3A, HBPE-CIDA$_1$ exhibits a three-dimensional (3D) spherical nano morphology, with an average diameter of 150 nm. In addition, larger nanospheres with the diameter of 200-300 nm could also be clearly observed, which shows the distribution of the particle sizes (Fig. S7). As a comparison, the TEM image of HBPE-CIDA$_4$ (Fig. 3B) exhibits a one-dimensional (1D) spindle-like

nano morphology. The length of the spindle is around 1.0 μm and the diameter of the cross-section is about 200 nm. Fig. 3C is a magnified TEM images of HBPE-CIDA$_4$ nanospindles. We suggest that the synergistic effect by multiple hydrogen bonds in the flexible cores among hydroxyl groups of the core and the π-π stacking interactions of peripheral CIDA groups stack in a face-to-face manner could be considered as the primary cause for the formation of spindle (Fig. 3F).[14-16] The 3D spherical-like structures exhibit larger micelles, which may be because the unimolecular micelles HBPE-CIDA$_1$ nanoparticles aggregate into approximate spherical large multimolecular micelles (Fig. 3E), most likely, driven by the intermolecular hydrogen bonds interactions among hydroxyl groups of the core. In this self-assembly process to form these special nanospindles, π-π stacking interactions and intermolecular hydrogen bonds like two or more lines strung the countless small HBPE-CIDA$_4$ nanoparticles together, then formed the stable one-dimensional nanospindles. Moreover, when a solution of HBPE-CIDA$_4$ exhibiting the special spindle-like morphology in ethyl acetate was stored at 4 °C for one month, no any change in size and morphology was observed (Fig. 3D), which indicated that the high stability of HBPE-CIDA$_4$ spindles.

The morphologies and the sizes of HBPE-CIDA$_1$ and HBPE-CIDA$_4$ nanoparticles were further established by SEM. As shown in Fig. 4A, HBPE-CIDA$_1$ has an average diameter of 1.5 μm which is a bit larger than the TEM test. This result further proves that HBPE-CIDA$_1$ nanospheres are easily aggregated for its strong intermolecular hydrogen bonds interactions. In addition, the size of HBPE-CIDA$_4$ nanospindles determined by SEM (1.0 μm) is highly consistent with that of TEM measurement (Fig. 4C).

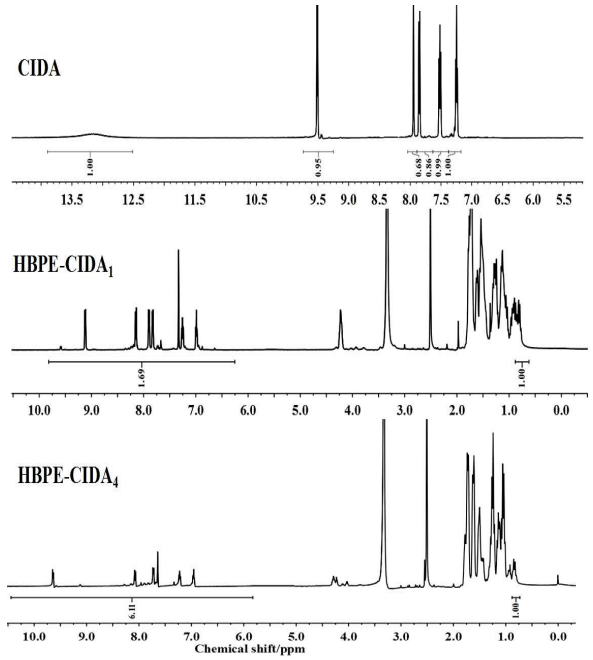

Fig. 2 ^{1}H NMR spectra of CIDA and HBPE-CIDA$_1$ and HBPE-CIDA$_4$

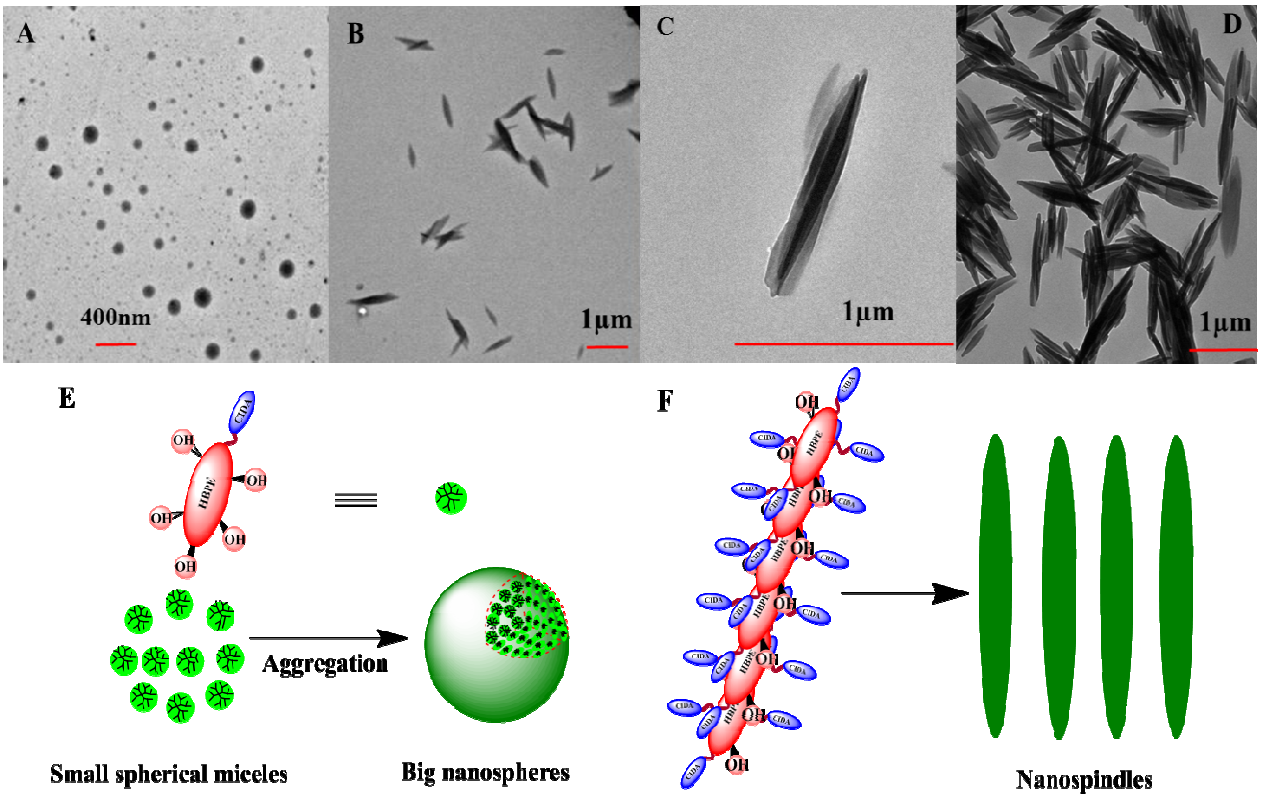

Fig. 3 (A) TEM images of HBPE-CIDA$_1$ nanospheres. (B) TEM images of HBPE-CIDA$_4$ nanospindles. (C) TEM images of the magnified HBPE-CIDA$_4$ nanospindles. (D) TEM images of the HBPE-CIDA$_4$ nanospindles in ethyl acetate solution (0.10 mg/mL) stored at room temperature for 30 days. (E) Molecular models of possible conformations and assemblies of HBPE-CIDA$_1$ nanospheres. (F) Molecular models of possible conformations and assemblies of HBPE-CIDA$_4$ nanospindles. All the samples were used as stock solutions in ethyl acetate solution (0.010 mg/mL) after treated by ultrasonic (100 Hz) for 5 min, and stored at room temperature for 1 hour.

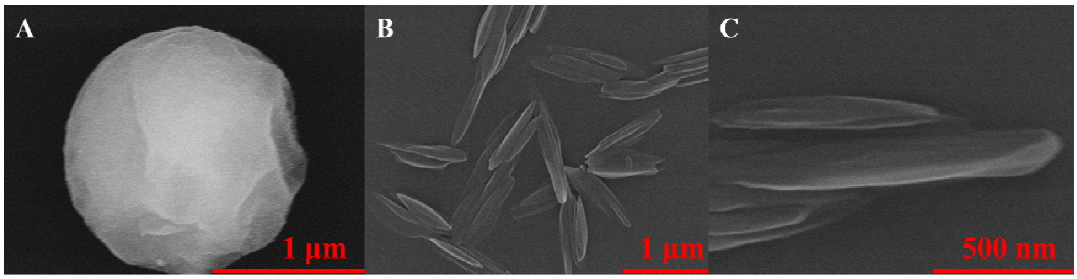

Fig. 4 (A) SEM images of HBPE-CIDA$_1$ nanospheres. (B) SEM images of HBPE-CIDA$_4$ nanospindles. (C) SEM images of the magnified HBPE-CIDA$_4$ nanospindles. All the samples were used as stock solutions in ethyl acetate solution (0.010 mg/mL) after treated by ultrasonic (100 Hz) for 5 min, and stored at room temperature for 1 hour.

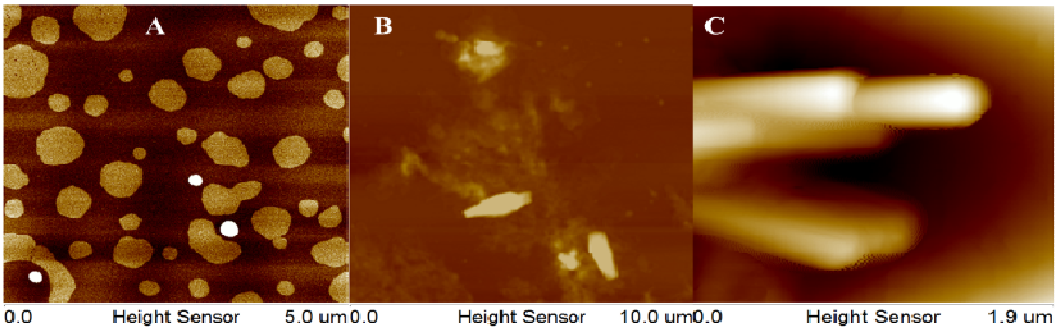

Fig. 5 Atomic force microscopy images of HBPE-CIDA$_1$ (A), HBPE-CIDA$_4$ (B) and the magnified layer of the HBPE-CIDA$_4$ (C).

To establish the surface morphology of the HBPE-CIDAs, atomic force microscopy (AFM) measurement was carried out. As shown in Figure 5A, HBPE-CIDA$_1$ has a spherical morphology with dispersive particle sizes and an average height of 1-2 nm (Fig. S8). While HBPE-CIDA$_4$ exhibits spindle-like morphology with a multilayered "onion-like" top surface (Fig. 5C).[15, 16, 23] The thickness of a single layer is approximately 3-4 nm (Fig. S9).

In addition, the X-ray diffraction data of the HBPE-CIDA$_1$ nanospheres shows a series of sharp peaks indicating an ordered structure in which the 1-cyanoindolizine terminal groups exhibit a certain extent of long-range order (Fig. 6, curve A). The strongest peak at 2θ = 17° corresponds to a d-spacing of 5.22 Å along the 1-cyanoindolizine molecules. The X-ray diffraction data from the nanospindles composed of HBPE-CIDA$_4$ also illustrates a series of much sharper peaks than HBPE-CIDA$_1$ (Fig. 6, curve B), which obviously indicate a highly ordered crystalline structure.[14, 16] The strongest peak at 2θ = 7.7° shows a longer d-spacing of 11.48 Å. It is worth noting that although HBPE-CIDA$_1$ also shows a series sharp peaks at 2θ = 7.7°, which are much weaker than that HBPE-CIDA$_4$, which suggests that HBPE-CIDA$_4$ nanospindles exhibits more organized nanostructures than HBPE-CIDA$_1$ nanospheres. These results are also in good consistent with the TEM, SEM and AFM spectra. The sharp diffraction peaks in each kind of sample once again proved that the well-ordered aggregate structure in the assemblies indeed exist.

Next, concerning the π-π conjugate structure of the modified CIDA groups, we investigated the fluorescence of CIDA, HBPE-CIDA$_1$ and HBPE-CIDA$_4$, respectively. Fluorescent spectra, digital camera image and fluorescent images of the CIDA, HBPE-CIDA$_1$ and HBPE-CIDA$_4$ in ethanol solution are showed in Fig. 7. At the same concentration, the HBPE-CIDA$_1$ nanospheres and CIDA showed the stronger fluorescence than HBPE-CIDA$_4$ nanospindles (order: HBPE-CIDA$_1$ ≈ CIDA > HBPE-CIDA$_4$). The reason of that HBPE-CIDA$_4$ shows the weak fluorescence than HBPE-CIDA$_1$ is closely related with its higher π-π stacking interactions of the peripheral CIDA groups.[23, 51]

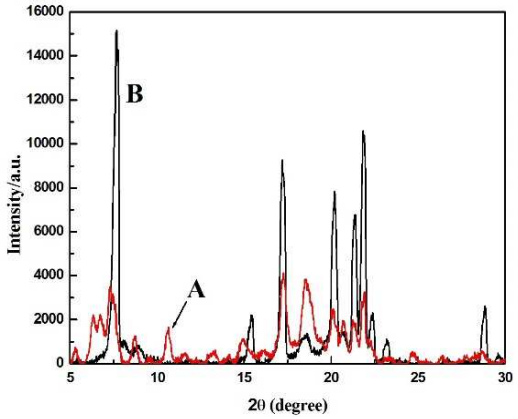

Fig. 6 X-ray diffraction data for nanparticles formed from (A) HBPE-CIDA$_1$ (red line) and (B) HBPE-CIDA$_4$ (black line)

To further study the fluorescence properties of HBPE-CIDA$_1$ and HBPE-CIDA$_4$, we first studied the influence of Fe^{3+} and other metal ions on the fluorescence intensity of CIDA. The influence of Fe^{3+} on the fluorescence intensity of the CIDA, HBPE-CIDA$_1$ and HBPE-CIDA$_4$ were evaluated by a fluorescence decreasement (FD = I/I_0) which was calculated by the ratio of the reduced fluorescence intensity in the presence of metal cations (I) and the fluorescence intensity without metal cations (I_0) shown in Fig. 8. From Fig. 8A, we find that CIDA shows selectively response to Fe^{3+}, only 6.6 × 10^{-5} M concentration of Fe^{3+} can decrease its fluorescence obviously.

Then we investigated the influence of Fe^{3+} and other metal ions on the fluorescence intensity of HBPE-CIDA$_1$ and HPBE-CIDA$_4$, which were showed in Fig.8 B, C respectively. From Fig. 8B, we know that HBPE-CIDA$_4$ almost showed no fluorescence response to all the tested metal ions, however the Fe^{3+} could make the fluorescence of the HBPE-CIDA$_1$ decreased to a certain extent, as shown in Fig. 8C. These two products with different nano morphologies showed different responses to Fe^{3+} which was probably because the HBPE-CIDA$_4$ spindles could not be easily affected by Fe^{3+} and other metal ions, for its structure was formed not only by the intermolecular hydrogen bonds among hydroxyl groups of the flexible core but also by the strong π-π stacking interactions of peripheral CIDA groups, while the HBPE-CIDA$_1$ nanospheres could be easily affected by Fe^{3+},[23] for its structure was formed mainly by intermolecular hydrogen bonds among hydroxyl groups of the flexible core and almost no π-π stacking interactions of peripheral CIDA groups. The order of the fluorescence responses to Fe^{3+} is HBPE-CIDA$_4$ < HBPE-CIDA$_1$ < CIDA, which is consistent with the theory that polymer aggregates exhibit high stability and durability than the small molecules, because of their mechanical and physical properties.[43] The complex of the HBPE-CIDA$_1$ with Fe^{3+} maybe trigger the mechanism of photoinduced electron transfer (PET) "OFF-ON" switching.[52] This is because, as usually observed, the electron transfer from the CN group to the excited state CIDA moiety quenches the emission.

In order to survey the π-π stacking interactions of the HBPE-CIDA$_4$, we assumed that whether those guest compounds such as naphthalene (NA), anthracene (AN) and pyrene (PY) with π-π conjugated structures will damage the π-π stacking interactions of the HBPE-CIDA$_4$. The effect of the fluorescent properties of HBPE-CIDA$_4$ with NA, AN and PY were studied respectively. The results showed that the addition of the NA almost had no effect on the fluorescence of HBPE-CIDA$_4$ (Fig. S10), and the addition of the PY could make its fluorescence enhanced slightly (Fig. S11). However, after addition of the AN, the emission intensity of HBPE-CIDA$_4$ enhanced about 4 times (Fig. 9A), while only 1.4 times for PY. Fig. 9B gave the real time fluorescence emission spectra of HBPE-CIDA$_4$ after the addition of AN, the high wavelength peaks at 400 nm enhanced. Fig. 9C presented the fluorescent spectra of AN, HBPE-CIDA$_4$ and HBPE-CIDA$_4$ with AN, compared with the same amount of AN and HBPE-CIDA$_4$ in ethanol, HBPE-CIDA$_4$ with AN showed much stronger fluorescent than the formers. It is supposed that fluorescence enhancement behaviors from AN is related with the fact that AN can exist between the two CIDA moieties as a pincer-like structure to separate two CIDA moieties which results in the rise of CIDA monomer fluorescence.[53] Because the conjugation degree of NA ring is poor than the AN ring, its conjugated structure is not enough to insert the two π-π stacking CIDA moieties of the HBPE-CIDA$_4$. Meanwhile, although PY is tend to be a pyrene excimer and the conjugation degree of it is better than the AN, due to its larger steric hindrance, it is hard to destroy the π-π stacking interactions of the HBPE-CIDA$_4$ either. As a comparison, the fluorescence behaviors of HBPE-CIDA$_1$ with NA, AN and PY were also studied respectively, they all showed negligible effects on the fluorescence intensity of HBPE-CIDA$_1$ (Fig. S12, Fig.S13 and Fig.S14). Through above fluorescent experiment, we further proved that the π-π stacking interactions of the HBPE-CIDA$_4$ were exactly exist, and this stable HPBE-CIDA$_4$ nanospindles was promising to be a potential fluorescent probe for selectively discriminating fused ring compounds, especially for AN.

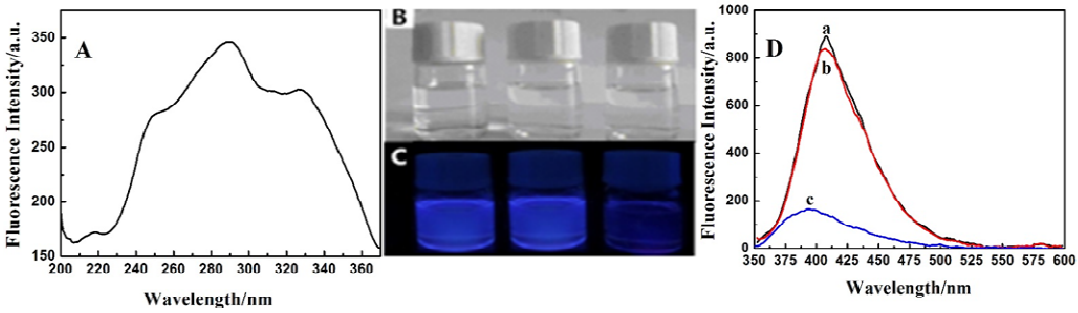

Fig. 7 (A) Fluorescence excitation spectra of the HBPE-CIDA$_1$. (B) The digital camera image of CIDA (left) and HBPE-CIDA$_1$ (middle) and HBPE-CIDA$_4$ (right) in ethanol solution under sunlight. (C) The fluorescent image of CIDA (left) and HBPE-CIDA$_1$ (middle) and HBPE-CIDA$_4$ (right) under UV light (λ= 260 nm), c = 2.0 × 10^{-5} M. (D) The fluorescence emission spectra of HBPE-CIDA$_1$ (a) and CIDA (b) and HBPE-CIDA$_4$ (c) in ethanol solution (c = 2.0 × 10^{-5} M, λ_{ex}= 290 nm, the excitation and emission slits are 5nm/2.5nm).

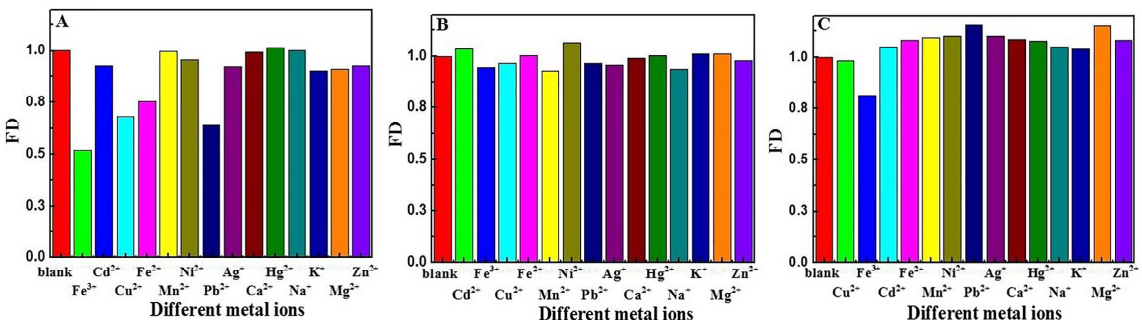

Fig.8 Fluorescence decreasement factors (FD) of the CIDA, λem = 410 nm (A), HBPE-CIDA$_4$, λem = 400 nm (B) and HBPE-CIDA$_1$, λem = 410 nm (C) (c = 2.0 × 10^{-5} M） in ethanol solution in the presence of Fe^{3+} at a concentration of 6.6× 10^{-5} M.

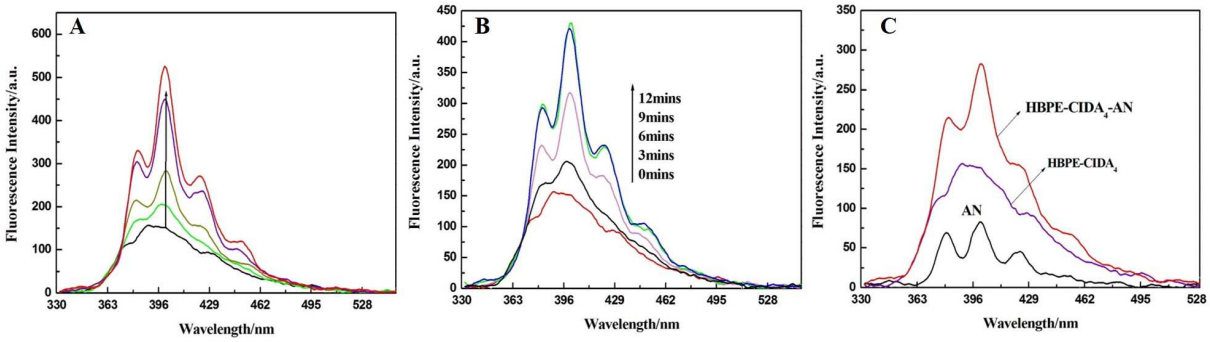

Fig.9 (A) Fluorescence emission spectra of HBPE-CIDA$_4$ in ethanol solution (c = 2.0 × 10^{-5} M) in the presence of AN at a concentration from 0 to 2.6 × 10^{-4} M. (B) Real time fluorescence emission spectra of HBPE-CIDA$_4$ (c = 2.0 × 10^{-5} M) after adding 1.3 × 10^{-4} M of AN. (C) Fluorescence emission spectra of AN, HBPE-CIDA$_4$ and HBPE-CIDA$_4$-AN. The concentrations of AN and HBPE-CIDA$_4$ were 1.3 × 10^{-4} M and 2.0 × 10^{-5} M respectively, λex = 290 nm.

In summary, herein we report a novel class of structural controllable nanohyperbranched polyesters functionalized with CIDA units, which could be synthesized by a facile one-pot procedure under mild reaction condition. The nano morphologies of the HBPE-CIDAs are closely related with their grafting rates of CIDAs. In addition, we found that the amplification of directional supramolecular interactions facilitated by the presence of multiple peripheral branches of even irregular, flexible molecules would lead to efficient self-assembly and formation of remarkably stable nanospindles. The results demonstrate that one-dimensional supramolecular assembling could be obtained by highly branched but irregular molecules without a tedious, multistep synthesis of the well-defined, shape-persistent molecules, while the three-dimensional supramolecular assembling could also be achieved by the less grafting rate of the periphery groups. On the other hand, such hyperbranched aromatic-aliphatic polyesters exhibit strong fluorescent intensity, different grafting rates, different nano morphologies and good solubilities. Furthermore, fluorescent experiments indicate that HBPE-CIDA$_4$ nanospindles is promising to serve as fluorescent probes for fused ring compounds, in particular, for the anthracene.

Notes and references

1. *Jiangsu Key Laboratory of Biofunctional Materials，Key Laboratory of applied photochemisty, School of Chemistry and Materials Science, Nanjing Normal University, Nanjing 210097(China).*

2. *Jiangsu Provincial Key Laboratory of Biomass Energy and Materials, National Engineering Laboratory for Biomass Chemical Utilization, Institute of Chemical Industry of Forest Products, CAF, Nanjing 210042 (China).*

Fax:86 025 85891397; Tel:86 025 85891397;

E-mail: hanqiaorong@njnu.edu.cn, wangbingxiang@njnu.edu.cn, mazhenye@njnu.edu.cn

† details of any supplementary information available should be included here

‡ Acknowledgements: We gratefully thank the financial support of the Priority Academic Program Development of Jiangsu Higher Education Institutions, the financial support of National Natural Science Foundation of China (No. 31400516) and the funding of the College Industrialization Project of Jiangsu Province (JHB2012-17).

1. H. K. Li, H. Q. Wu, E. G. Zhao, J. Li, J. Z. Sun, A. J. Qin and B. Z. Tang, *Macromolecules,* 2013, **46**, 3907−3914.
2. A. J. Qin, J. W. Y. Lam, H. C. Dong, W. X. Lu, C. K. W. Jim, Y. Q. Dong, M. Ha1ussler, H. H. Y. Sung, I. D. Williams, G. K. L. Wong and B. Z. Tang, *Macromolecules*, 2007, **40**, 4879−4886.
3. J. Wang, J. M, E. G. Zhao, Z. G. Song, A. J. Qin, J. Z. Sun and B. Z. Tang, *Macromolecules,* 2012, **45**, 7692−7703.
4. Z. Li, J. W. Y. Lam, Y. Q. Dong, Y. P. Dong, H. H. Y. Sung, I. D. Williams and B. Z. Tang, Macromolecules, 2006, **39**, 6458−6466.
5. A. Sidorenko, X. W. Zhai, A. Greco and V. V. Tsukruk, *Langmuir,* 2002, **18**, 3408−3412.
6. A. Sidorenko, X. W. Zhai, S. Peleshanko, A. Greco, V. V. Shevchenko and V. V. Tsukruk, *Langmuir*, 2001, **17**, 5924−5931.
7. R. J. Dong, B. S. Zhu, Y. F. Zhou, D. Y. Yan and X. Y. Zhu, *Angew. Chem. Int. Ed*., 2012, **51**, 11633 –11637.
8. J. Y. Liu, Y. Pang, W. Huang, X. Zhai, X. Y. Zhu, Y. F. Zhou and D. Y. Yan, *Macromolecules*, 2010, **43**, 8416–8423.
9. W. Tao, Y. Liu, B. B. Jiang, S. R. Yu, W. Huang, Y. F. Zhou and D. Y. Yan, *J. Am. Chem. Soc*., 2012, **134**, 762−764.
10. Q. R. Han, X. H. Chen, Y. L. Niu, B. Zhao, B. X. Wang, C. Mao, L. B. Chen and J. Shen, Langmuir, 2013, **29**, 8402−8409.
11. A. Z. Samuel and S. Ramakrishnan, *Macromolecules*, 2012, **45**, 2348−2358.
12. J-K Kim, E. Lee, Z. G. Huang and M. Lee, *J. Am. Chem. Soc*., 2006, **128**, 14022−14023.
13. B. R. Yu, B. Y. Wang, S. W. Guo, Q. Zhang, X. R. Zheng, H. T. Lei, W. S. Liu, W. F. Bu, Y. Zhang and X. Chen, *Chem. Eur. J*., 2013, **19**, 4922 – 4930.
14. M. Ornatska, S. Peleshanko, B. Rybak, J. Holzmueller and V. V. Tsukruk, *Adv, Mater*., 2004, **16**, 23−24.
15. M. Ornatska, K. N. Bergman, M. Goodman, S. Peleshanko, V. V. Shevchenko and V. V. Tsukruk, *Polymer*, 2006, **47**, 8137−8146.
16. M. Ornatska, S. Peleshanko, K. L. Genson, B. Rybak, K. N. Bergman and V. V. Tsukruk, *J. Am. Chem. Soc*., 2004, **126**, 9675−9684.
17. Z. P. Wang, H. Möhwald and C. Y. Gao, *ACS Nano.*, 2011, **5** (5), 3930–3936.
18. F. M. Xu, H. B. Wang, J. Zhao, X. S. Liu, D. D. Li, C. J. Chen and J. Ji, *Macromolecules*, 2013, **46**, 4235−4246.
19. D. Lanson, M. Schappacher, A. Deffieux and R. Borsali, *Macromolecules*, 2006, **39** (20), 7107–7114.
20. H. D. Selby, B. K. Roland and Z. P. Zheng, *Acc. Chem. Res*., 2003, **36**, 933−944.
21. H. B. Li, A. G. Kanaras and L. Manna , *Acc. Chem. Res*., 2013, **46** (7), 1387−1396.
22. Z. L. Su, B. Yu, X. S. Jiang and J. Yin, *Macromolecules*, 2013, **46**, 3699−3707.
23. Q. R. Han, Y. L. Jiang, C. Jin, S. S. Cheng, X. X. Wang, X. Y. Wang and B. X. Wang, *Polym. Chem*., 2014, **5**, 5900−5905.
24. B. M. Rosen, C. J. Wilson, D. A. Wilson, M. H. Peterca, M. R. Imam, and V. Percec, *Chem. Rev*., 2009, **109**, 6275–6540.
25. V. Percec, M. R. Imam, M. H. Peterca, D. A. Wilson and P. A. Heiney, *J. Am. Chem. Soc*., 2009, **131**, 1294−1304.
26. G. B. Sun, J. Hentschel and Z. B. Guan, *ACS Macro Lett*., 2012, **1**, 585−588.
27. J. Y. Liu, Y. Pang, W. Huang, X. H. Huang, L. L. Meng, X. Y. Zhu, Y. F. Zhou and D. Y. Yan, *Biomacromolecules*, 2011, **12** (5), 1567–1577.
28. Z. P. Guo, Y. H. Li, H. Y. Tian, X. L. Zhuang, X. S. Chen and X. B. Jing, *Langmuir*, 2009, **25** (17), 9690–9696.

29. Y. Liu, C. Y. Yu, H. B. Jin, B. B. Jiang, X. Y. Zhu, Y. F. Zhou, Z. Y. Lu and D. Y. Yan, *J. Am. Chem. Soc*., 2013, **135** (12), 4765–4770.
30. J. Y. Liu, W. Huang, Y. Pang, X. Y. Zhu, Y. F. Zhou and D. Y. Yan, *Langmuir*, 2010, **26** (13), 10585–10592.
31. C. M. Yu, Y. L. Wu, F. Zeng, X. Z. Li, J. B. Shi and S. Z. Wu, *Biomacromolecules*, 2013, **14**, 4507−4514.
32. S. Santra, C. Kaittanis and J. Manuel Perez, *Langmuir*, 2010, **26**, 5364–5373.
33. R. Reul, J. Nguyen and T. Kissel, *Biomaterials*, 2009, **30**, 5815–5824.
34. M. R. Rekha, C. P. Sharma, *Biomaterials*, 2009, **30**, 6655–6664.
35. J. Y. Liu, Y. Pang, W. Huang, X. Y. Zhu, Y. F. Zhou and D. Y. Yan, *Biomaterials*, 2010, **31**, 1334–1341.
36. N. A. A. Rossi, I. Constantinescu, R. K. Kainthan, D. E. Brooks, M. D. Scott and J. N. Kizhakkedathu, *Biomaterials*, 2010, **31**, 4167–4178.
37. C. Mugabe, R. T. Liggins, D. Guan, I. Manisali, I. Chafeeva, D. E. Brooks, M. Heller, J. K. Jackson and H. M. Burt, *Int. J. Pharm*., 2011, **404**, 238–249.
38. R. J. Dong, Y. F. Zhou and X. Y. Zhu, *Acc. Chem. Res*., 2014, **47**, 2006−2016.
39. P. Huang, D. L. Wang, Y. Su, W. Huang, Y. F. Zhou, D. X. Cui, X. Y. Zhu and D. Y. Yan, *J. Am. Chem. Soc*., 2014, **136**, 11748−11756.
40. S. R. Yu, R. J. Dong, J. X. Chen, F. Chen, W. F. Jiang, Y. F. Zhou, X. Y. Zhu and D. Y. Yan, *Biomacromolecules*, 2014, **15**, 1828−1836.
41. K. D. Anderson, K. Marczewski, S. Singamaneni, J. M. Slocik, R. Jakubiak, R. R. Naik, T. J. Bunning and V. V. Tsukruk, *ACS. Applied Materials & interfaces*, 2010, **2** (8), 2269–2281.
42. G. Fernández, L. Sánchez, E. M. Pérez and N. Martín, *J. Am. Chem. Soc*., 2008, **130**, 10674–10683.
43. D. H. Zhang, Z. C. Xu, J. Li, S. F. Chen, J. Cheng, A. Q. Zhang, S. H. Chen and M. H. Miao, *ACS Appl. Mater. Interfaces*, 2014, **6**, 16375−16383.
44. X. H. Zeng, Y. N. Zhang and A. M. Nyström, *Biomacromolecules*, 2012, **13**, 3814−3822.
45.W. Y. Dong, C. L. Tu, W. Tao, Y. F. Zhou, G. S. Tong, Y. L. Zheng, Y. J. Li and D. Y. Yan, *Cryst. Growth De.,* 2012, **12**, 4053−4059.
46. S. W, J. Zhang, L. H. Shi, S. X. Tang, Y. G. Li, L. N. Jiang and Q. L. Cui, *RSC Adv*., 2014, **4**, 8209–8215.
47. F. Xiang, M. Stuart, J. Vorenkamp, S. Roest, H. Timmer-Bosscha, M. C. Stuart, R. Fokkink and T. Loontjens, *Macromolecules*, 2013, **46**, 4418−4425.
48. H. H. Cai, G. L. Jiang, C. Y. Chen, Z. B. Li, Z. H. Shen and X. H. Fan, *Macromolecules*, 2014, **47**, 146−151.
49. J. P. Michael, *Nat. Prod. Rep*., 2008, **25**, 139–165.
50. F. Delattre, P. Woisel, G. Surpateanu, F. Cazier and P. Blach, *Tetrahedron*, 2005, **61**, 3939–3945.
51. L. Song, C. L. Tu, Y. F. Shi, F. Q. Qiu, L. He, Y. Jiang, Q. Zhu, B. S. Zhu, D. Y. Yan and X. Y. Zhu, *Macromol. Rapid Commun*., 2010, **31**, 443–448.
52. G. J. Zhang, H. Y. Li, S. M. Bi, L. F. Song, Y. X. Lu, L. Zhang, J. J. Yu and L. M. Wang, *Analyst*, 2013, **138**, 6163–6170.
53. Z. C. Xu, N. J. Singh, J. Lim, J. Pan, H. N. Kim, S. Park, K. S. Kim and J. Y. Yoon, *J. Am. Chem. Soc*., 2009, **131**, 15528–15533.

Graphical Abstract

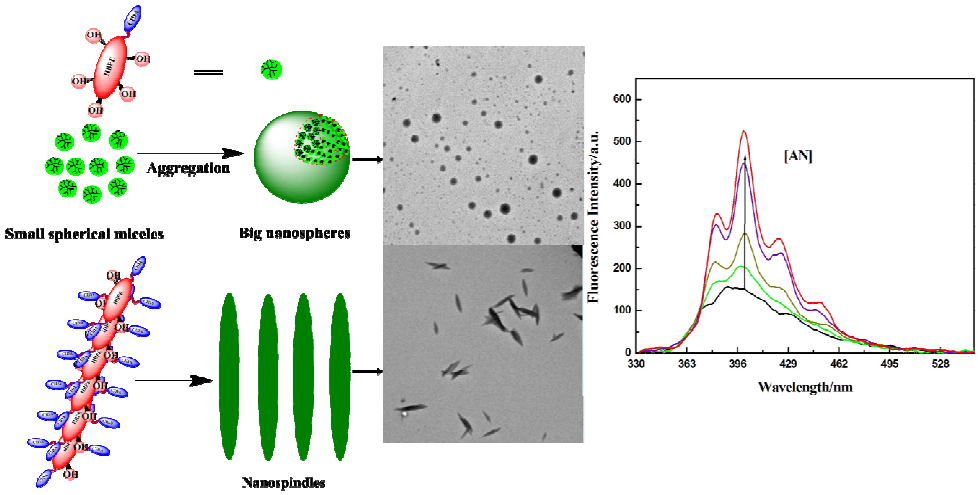

Two novel functionalized hyperbranched aromatic-aliphatic co-polyester nanoparticles of HBPE-CIDA$_1$ and HBPE-CIDA$_4$ were synthesized by modifying periphery of the second generation hyperbranched polyester (HBPE) with 1-cyanoindolizine-3-carboxylic acid (CIDA) groups via one-pot synthesis method. Such hyperbranched nanospheres and nanospindles exhibited strong fluorescent intensity, different grafting rates, different nano morphologies. Interestingly, higher grafted HBPE-CIDA$_4$ nanospindles was established to be a highly sensitive fluorescent sensor for anthracene .